Journal of Civil Engineering and Construction 2019;8(4):137-148
https://doi.org/10.32732/jcec.2019.8.4.137

Numerical Study on Uniaxial Compression Behavior of Geobags

N. Hataf*, M. Javahery
Department of Civil and Environmental Engineering, Shiraz University, Shiraz, Iran
E-mail: nhataf@shirazu.ac.ir (Corresponding author)

Received: 21 June 2019; Accepted: 24 August 2019; Available online: 30 September 2019

Abstract: Geobags have been used as coastal erosion control and flood preventing measures during the last decades. More recently engineers have used geobags to improve the bearing capacity of soft soils. In this paper, a study was performed to investigate the behavior of geobags under compression loadings utilizing a finite element computer software. The numerical modeling was verified by simulating reported laboratory compression test results. The effects of various parameters such as geobag's dimensions, mechanical characteristics of filling soil and bag material properties on the ultimate bearing capacity of geobags were investigated. It was shown that increasing the friction angle of filling soil and the tensile strength of textile lead to an increase in the geobag ultimate compressive load capacity. On the other hand, an increase in dilation angle of filling soil, Poisson's ratio and the height of geobag lead to a decrease in the ultimate compressive load capacity of geobags.
Keywords: Geobag; Analytical analysis; Finite Element Method; Compressive load capacity.

1. Introduction

Geobag is a three-dimensional geosynthetic container (i.e. bag) made of textile fabric with sufficient tensile strength filled with soil, crushed rock, recycled concrete, etc. and used as temporary or permanent earth structure. Flexible bags are made of Polyethylene (PE) or Polypropylene (PP). Use of geobags for coastal erosion control, flood-preventing measures has been known to engineers for decades. Geobag, in its present form, was developed in the Netherlands and used in the construction of riverbanks in the Rhine to control the flow direction in 1986 [1]. Since geobags are economical and easy to make, they have soon found many other applications in civil engineering projects, in many countries, all around the world [2-6]. Geotextile, due to its durability, stability, performance and simplicity in construction of geobag is usually used as container. Soil improvement with geobags has many technical and economic advantages compared to other reinforcement methods [2, 3]. More recently, geobags have been used to improve the bearing capacity of soft soils. Besides, the ability of geobag infilling soil to dissipate excess pore water pressure generated in the surrounding soil, due to the high permeability, during dynamic loading or earthquake can reduce the risk of liquefaction. To achieve a better understanding of the behavior of geobags in this regard, in the present study, the effects of bag material properties, the geometry of the bag and filling soil characteristics on the compression load capacity of geobags are investigated.

2. Previous studies

Stress and strain relationship for geobags under compression loading was investigated by Matsuoka [2]. Matsuoka and Liu studied geobags as reinforcing elements to increase the bearing capacity of foundations through laboratory testing [3]. Failure mechanisms and deformations of geobags were examined by Aqil et al. [4]. Experimental study on geobags' shear strength and their behavior under normal stress were conducted by Lohani et al. [5]. They also studied the effect of various parameters such as filling material type, number of bags and different texture of bags material on geobags bearing capacity. Geobag's apparent cohesion in two-dimensional space under direct compression test was introduced by Xu et al. [6]. They presented the load-displacement and stress-strain diagrams and obtained the bearing capacity of geobags mat using the plate load test results. Based on geobags' mechanical behavior and assuming frictionless and interlocked interfaces between the filling material and the bag, the ultimate strength of geobags were investigated [7]. The consolidation rate of clay-filled geotextile bags was explored under confining pressure [8]. Three-dimensional (3-D) numerical analysis was applied on geobags under static and dynamic normal loads and results were compared to two-dimensional (2-D) relations for apparent cohesion [9]. Hosseini and Hataf studied the effect and efficiency of geomats on reducing bridge pier abutment's scour [10]. It showed that geobags are environmentally friendly and can be used to reduce traffic-induced vibration or vibration due to seismic loading [2]. It was also found that bags made of PE or PP are stable

against both acids and alkali. Furthermore, bags are very durable if protected from exposure to sunlight via burying. New geosynthetic fabrics, however, are produced with high strengths and resistance to abrasion, puncture, tear and ultraviolet deterioration. More recently, the use of geobags to improve the bearing capacity of soft soils attracting researcher's attention. Matsuoka and Liu reported that geobags have high compressive strength (up to nearly 3 MPa-approximately one-tenth that of usual concrete) and increase the bearing capacity of soft ground 5-10 times [2]. The bearing capacities of shallow foundations on reinforced soil using geobags under vertical loads were determined experimentally and numerically by Hataf and Sayadi [11]. Results of their study showed that using geobags under footings significantly increases the bearing capacity of the foundation. It was also found that the number and arrangement of geobags are the most important factors in the increase of bearing capacity and decrease of settlements of foundations. In a study, Liu et al. used geobags to construct a retaining wall and found they have high compressive strengths resulting from the tensile forces of woven bags [12].

3. Theoretical analysis

Deformation and strength properties of a 2D model for geobag were studied by Chen [13]. Deformations in geobags under normal loads cause tensions in the bag. Chen introduced an apparent cohesion, C_a, for filling soil material due to the confinement effect of the bag. Apparent cohesion is defined as the amount of cohesion, C_a, which is added to soil inherent cohesion, C_s, increasing the total cohesion, C_g, of soil bag system to $C_g = C_s + C_a$.

The ultimate compressive strength of geobag is obtained using the following equations [14]:

$$\sigma_1 = K_p\sigma_3 \ \rightarrow \sigma_{1f} + \Delta\sigma_1 = K_p(\sigma_{3f} + \Delta\sigma_3) \ \rightarrow \sigma_{1f} + \Delta\sigma_1 = K_p\Delta\sigma_3 \quad (1)$$

where σ_1 and σ_3 are representing maximum and minimum principal stresses in filling soil, respectively. σ_{1f} and σ_{3f} are external stresses on geobag. $\Delta\sigma_1$ and $\Delta\sigma_3$ are average of excess stresses due to tension in geobag and K_p is Rankine's passive earth pressure coefficient. For uniaxial compression loading $\sigma_3 = \sigma_{3f} = 0$. Using the Mohr-Coulomb failure criterion, we have:

$$\sigma_{1f} = K_p\sigma_{3f} + 2C_a\sqrt{K_p} \rightarrow \sigma_{1f} = 2C_a\sqrt{K_p} \quad (2)$$

Substituting equation (1) in equation (2) the apparent cohesion can be obtained as:

$$C_a = \frac{K_p\Delta\sigma_3 - \Delta\sigma_1}{2\sqrt{K_p}} \quad (3)$$

Deformations in geobags under normal loads cause tension, T, which causes extra stresses in geobags. $\Delta\sigma_1$ and $\Delta\sigma_3$ are derived from the integration of these tensile force in unit width [14]. In the cited relation (i.e. equation 3) for apparent cohesion, only maximum and minimum principal stresses were used. To introduce intermediate principal stresses, σ_2, Drucker-Prager yield criterion may be used as follows:

$$\sqrt{\frac{1}{6}[(\sigma_1 - \sigma_2)^2 + (\sigma_2 - \sigma_3)^2 + (\sigma_3 - \sigma_1)^2]} = \alpha(\sigma_1 + \sigma_2 + \sigma_3) + \beta \quad (4)$$

where, $\alpha = \frac{2\sin\emptyset}{\sqrt{3}(3-\sin\emptyset)}$ and $\beta = \frac{6c\cos\emptyset}{\sqrt{3}(3-\sin\emptyset)}$.

For uniaxial compression loading at failure, we have:

$$\sigma_{2f} = \sigma_{3f} = 0 \quad (5)$$

To calculate the external stresses on geobags in ultimate condition, equation (4) may be rewritten as:

$$\frac{1}{\sqrt{3}}\sigma_{1f} = \alpha\,\sigma_{1f} + \beta_a \rightarrow \sigma_{1f} = \frac{\beta a}{\frac{1}{\sqrt{3}} - \alpha} \quad (6)$$

On the other hand, deformations of geobags under normal loads cause tension, T, which engenders extra stresses in geobags. By considering the uniform tension stress in all directions (i.e. $T_1 = T_2 = T_3$) and equal to the ultimate tensile strength of bag material (T) we have:

$$\Delta\sigma_1 = \frac{T_1\,(2L+2B)}{BL} = \frac{2T_1}{L} + \frac{2T_1}{\mathrm{B}} \rightarrow \Delta\sigma_1 = \frac{2T}{L} + \frac{2T}{\mathrm{B}} \quad (7)$$

$$\Delta\sigma_2 = \frac{T_2(2H+2B)}{BH} = \frac{2T_2}{H} + \frac{2T_2}{\mathrm{B}} \rightarrow \Delta\sigma_2 = \frac{2T}{H} + \frac{2T}{\mathrm{B}} \quad (8)$$

$$\Delta\sigma_3 = \frac{T_3(2L+2H)}{LH} = \frac{2T_3}{L} + \frac{2T_3}{\mathrm{H}} \rightarrow \Delta\sigma_3 = \frac{2T}{L} + \frac{2T}{\mathrm{H}} \quad (9)$$

where L is the length, B is width and H is the height of geobag. The confinement effect of geobag is therefore related to tension stresses developed in bag material.

4. Numerical modeling

To investigate the behavior of geobags a commercially available 3-D finite element code (ABAQUS) [15] was employed for modeling geobags. The model composed of three parts: soil, geobag, loading plates, as shown in Fig. 1-a).

Mohr-Coulomb plastic failure criterion was used to investigate the behavior of fill soil in geobag. Tetrahedral elements were used to model the soil. Square elements were used for loading plates. Plates were loaded and stresses, strains and load-settlements curves were obtained numerically for each test and used for further analysis. Typical numerical model using the input parameters is illustrated in Table 1 and results are shown in Figs. 1-b) and 1-c). In Fig. 1-b) the maximum principal stresses developed in geobag are shown. As it can be seen, stresses distribute at center and corners of geobag. The von Mises stresses developed in the soil are shown in Fig. 1-c). The maximum stresses are observed at the mid part of soil, as it is expected.

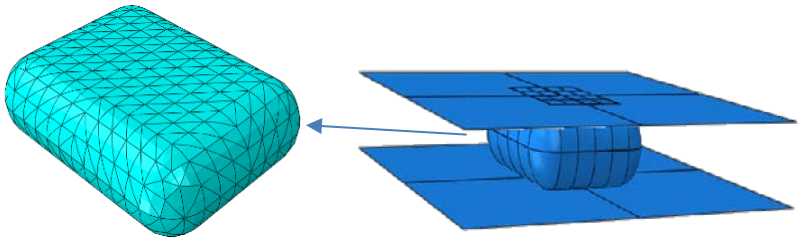

a) Numerical model of plates and geobag

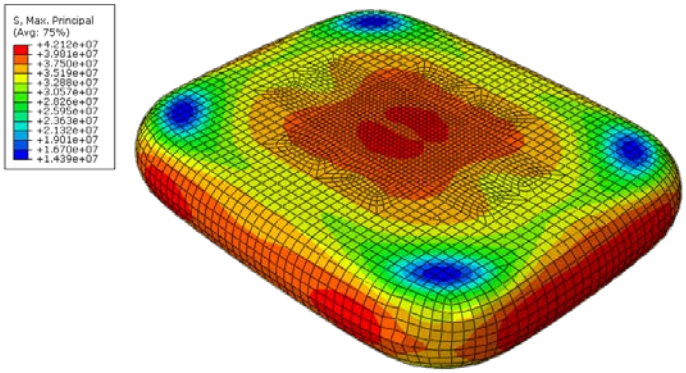

b) Stresses in the geotextile (kN/m^2)

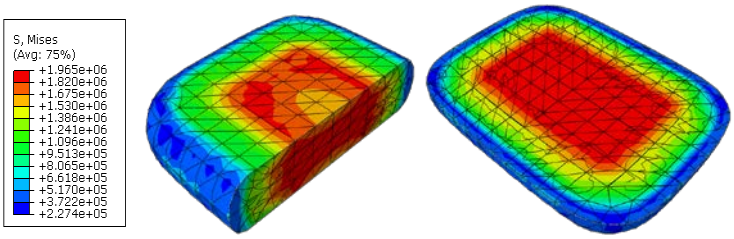

c) Stresses in the soil (kN/m^2)

Fig. 1. Numerical modeling and analysis results of geobag system under compression

The model, then, has been verified using experimental test results reported by Xu et al. [6]. The input parameters according to Xu et al. [6], used for numerical modeling are illustrated in Table 1. The numerical results are compared with experimental results and shown in Fig. 2. As seen the agreement between the numerical results and measured values are acceptable.

Table 1. Parameters of soil and bag material used in model verification

Parameter	Values	Description
ν_s	0.3	Poisson's ratio of soil
Es (MPa)	4	Young's Modulus of soil
Eg (MPa)	384	Young's Modulus of bag material
T (MPa)	23	Ultimate tensile strength of bag material
φ°	44	Friction angle of soil
ψ°	6	Dilation angle of soil
B (cm)	36	Width of geobag
L (cm)	46	Length of geobag
H (cm)	14	Height of geobag
φsg°	40	Soil-geotextile interaction friction angle
φpg°	26	Plate-geotextile interaction friction angle

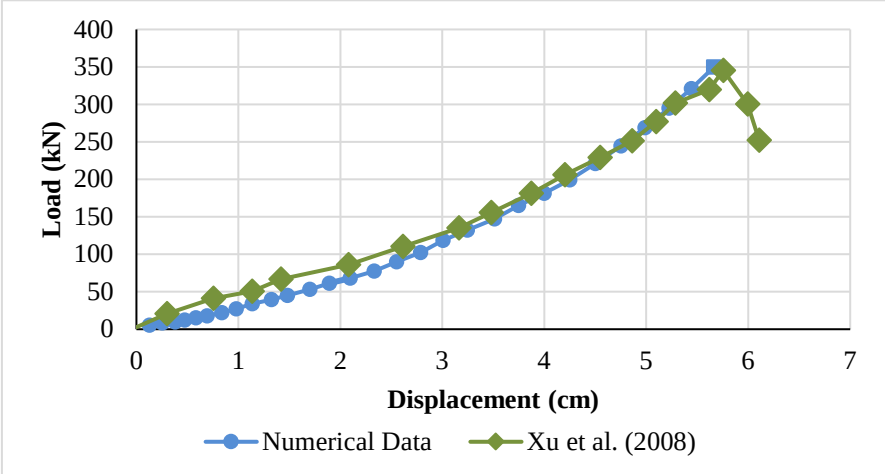

Fig. 2. Comparison of numerical modeling and experimental data

5. Parametric study of geobag compression capacity

Having verified the accuracy of numerical modeling, the effect of significant parameters on the ultimate uniaxial compression strength of geobag was investigated. These parameters are width and height of geobag, modulus of elasticity, Poisson's ratio, friction angle, and dilation angle of filling soil and tensile strength of bag material. The effects of these parameters on geobag compression strength have not been studied numerically in 3D modeling in previous researches. Poisson's ratios of soil were changed from 0.1 to 0.49. The modulus of elasticity of filling soil was changed from 4 to 150 MPa, friction angle was changed from 6 to 44 degrees and cohesion of soil was considered equal to zero. The Young's Modulus of bag material was changed from 61 to 1200 MPa. The ultimate tensile strength of bag material was varied from 28 to 190 MPa. Width of geobag was varied from 26 to 46 cm and height of geobag was changed from 10 to 22 cm. These dimensions were chosen to cover the dimensions of geobags used in laboratory and field. Soil and bag material properties used in numerical analysis are shown in Table 2 in detail. In each analysis, the values of all other parameters required were chosen according to Xu et al. [6] data, Table 1. The parameter under consideration is then changed according to Table 2.

The ultimate strength of geobag was determined from the load-settlement curve obtained numerically. There are two methods used to determine the ultimate load capacity, including peak point method and strain level method. In the first method, (i.e. peak point method) the ultimate load capacity is defined as the load obtained at the peak point of the load-displacement curve. In the second method, the loads corresponding to normal strain levels (i.e. u/H, where u is vertical deformation and H is the initial height of the geobag), equal to 10%, 15%, and 30% were considered as the load capacity of geobag. In both methods, the load is divided by geobag plan area to obtain distributed load capacity of geobag.

Table 2. Parameters of soil and bag material used in the parametric study

Parameter	Values	Description
ν_s	0.1, 0.2, 0.3, 0.38, 0.42, 0.46, 0.49	Poisson's ratio of soil
Es (MPa)	4, 5, 6, 7, 9, 11, 13, 15, 25, 35, 45, 60, 70, 85, 100, 125, 150	Young's Modulus of soil
Eg (MPa)	61, 92, 182, 372, 1200	Young's Modulus of bag material
T (MPa)	28, 37, 55, 100, 145, 190	Ultimate tensile strength of bag material
φ°	6, 14, 24, 34, 44	Friction angle of soil
ψ°	6, 14, 24, 34, 44	Dilation angle of soil
B (cm)	26, 31, 36, 41, 46	Width of geobag
L (cm)	46	Length of geobag
H (cm)	10, 14, 18, 22	Height of geobag

5.1 Effect of geobag's width

The effect of geobag's width on the ultimate load and distributed load capacity of geobag using the first method is illustrated in Figs. 3a and 3b, respectively. In the latter figure, the vertical axis indicates the peak normal stress carried by geobags. As seen an optimum width is obtained for the parameters used in this study. The effect of geobag's width on the ultimate strength of geobag at different normal strain levels is demonstrated in Fig. 4. Despite the first case, in this method, the distributed load capacity shows no peak value with the bag's width at strain levels is examined.

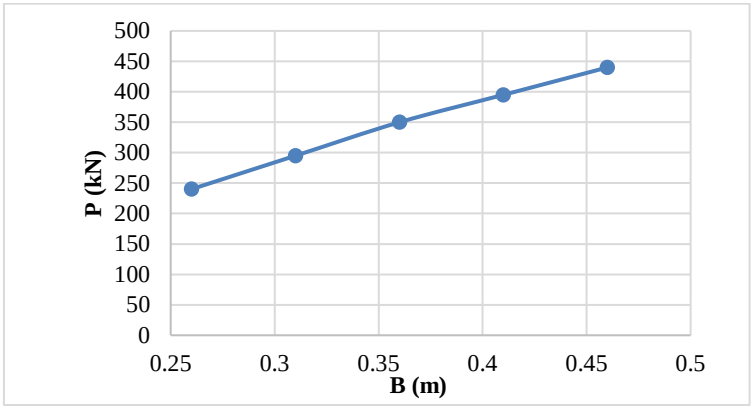

a)

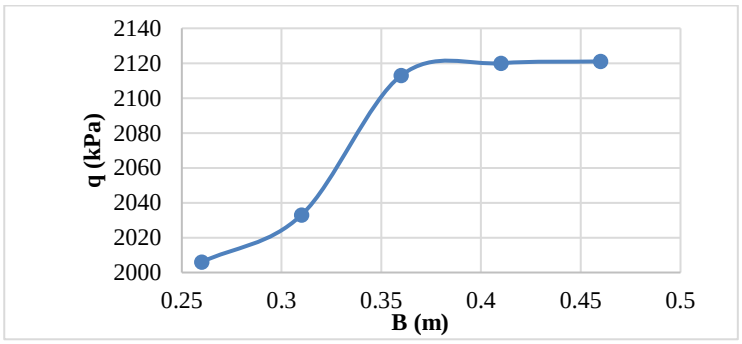

b)

Fig. 3. The effect of geobag's width on ultimate strength (peak point method); a) Load Capacity, b) distributed load capacity

5.2 Effect of geobag's height

The effect of geobag's height on the ultimate compression load capacity of geobags is shown in Figs. 5 and 6. As seen, increasing the height of geobag leads to a decrease in the ultimate load capacity of geobag. In Fig. 7 the effect of the increase of geobag's height on ultimate displacement determined by the peak point method is shown. According to this figure increase in geobag's height leads to a decrease in geobag's settlement. This might be attributed to the decrease in confining pressure within the soil embedded in the bag with an increase in geobag height.

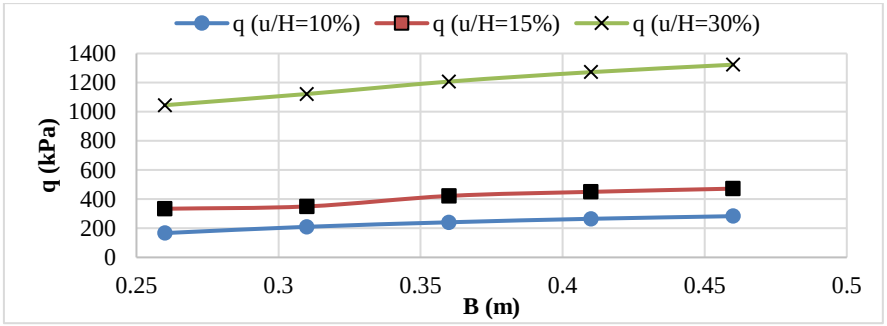

Fig. 4. The effect of geobag's width on compressive strength at different strain levels (u/H=10%, 15%, 30%)

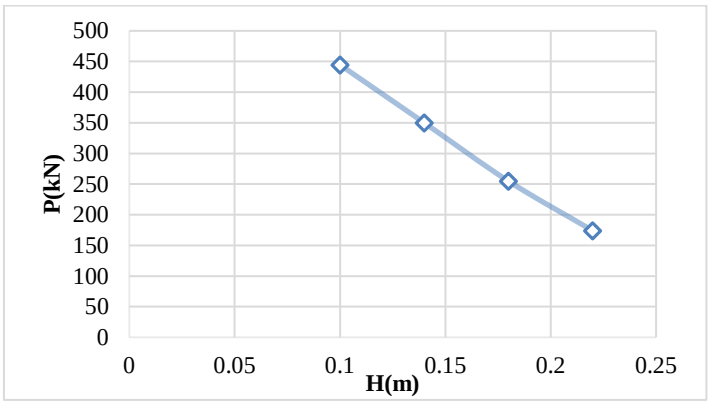

Fig. 5. The effect of geobag's height on the ultimate compression load capacity of geobags (peak point method)

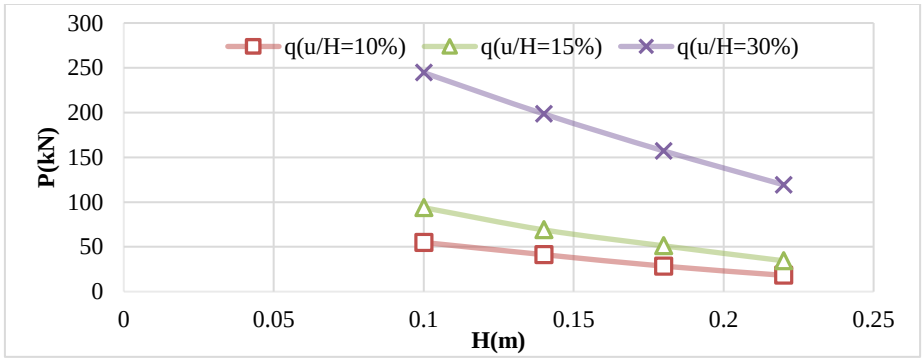

Fig. 6. The effect of geobag's height on the ultimate compression load capacity of geobags at different normal strain levels (u/H=10%, 15%, 30%)

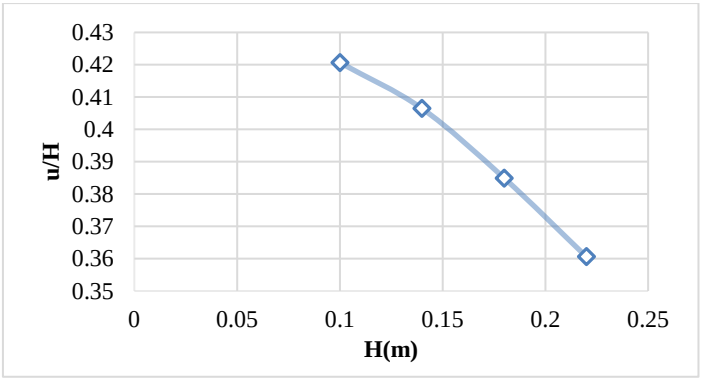

Fig. 7. The effect of the increase of geobag's height on ultimate normal displacement (peak point method)

5.3 The effect of friction angle of filling soil

Influence of friction angle of filling soil on ultimate load capacity and load at different normal strain levels is illustrated in Figs. 8 and 9. According to these figures, as expected the ultimate load capacity and loads at different

strain levels increased by increasing friction angle. This is because of the apparent cohesion, increase due to an increase in the Rankine passive coefficient, as it was shown in two-dimensional relation of apparent cohesion (equation 3). Fig. 10 shows the effect of friction angle of filling soil on the ultimate displacement of geobag determined using the peak point method. As it can be seen the ultimate displacement increased by increasing the friction angle of filling soil.

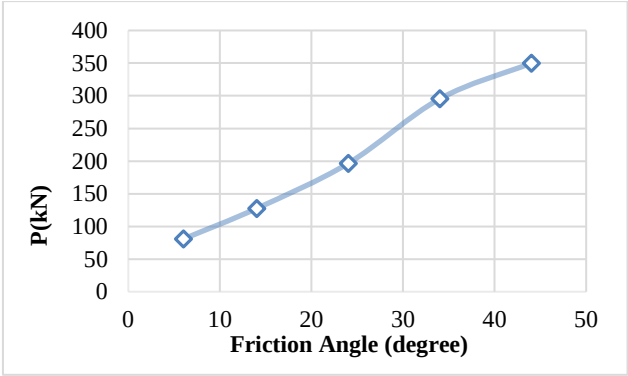

Fig. 8. Influence of friction angle of filling soil on ultimate load capacity (peak point method)

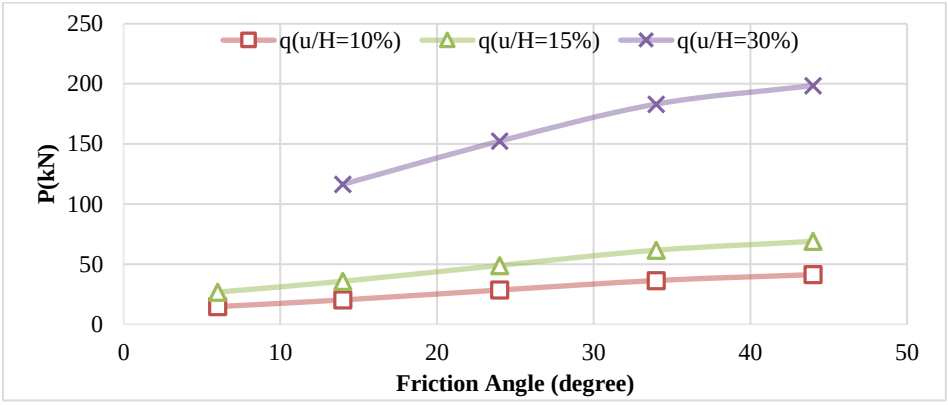

Fig. 9. Influence of friction angle of filling soil on the load at different normal strain levels (u/H=10%, 15%, 30%)

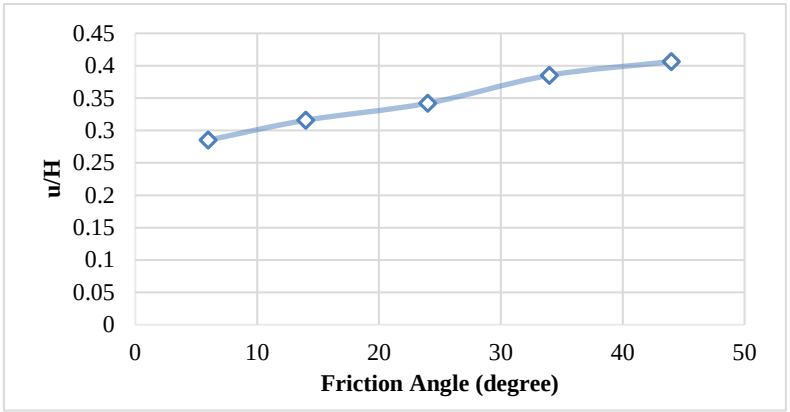

Fig. 10. The effect of the friction angle of filling soil on the ultimate displacement (peak point method)

5.4 The effect of the dilation angle of filling soil

The effect of changing the dilation angles of filling soil on the volumetric strain of geobag (ε_v) is illustrated in Fig. 11. As it is depicted in this figure, the volumetric strain of the geobag slightly decreases due to an increase in dilation angle. This is because the overall increase in dilation angle causes the increase in volume due to the shear strain created in filling soil under loading. The ultimate load capacity with respect to the dilation angle is shown in Fig. 12. It is shown in this figure that the ultimate load decreases due to an increase in dilation angle. The effect of the dilation angle of filling soil on the load at different normal strain levels is illustrated in Fig. 13. As shown, an increase in dilation angle causes a slight increase in ultimate loads and load capacity at different strain levels.

This might be due to a volume increase of geobags during loading condition, hence, increasing the area of geobag's contact with loading plate and experiencing more applied pressure. Fig. 14 represents the effect of the dilation angle on the ultimate displacement using the peak point method. Settlement in the geobags has slightly decreased at ultimate loads due to increase in dilation angle.

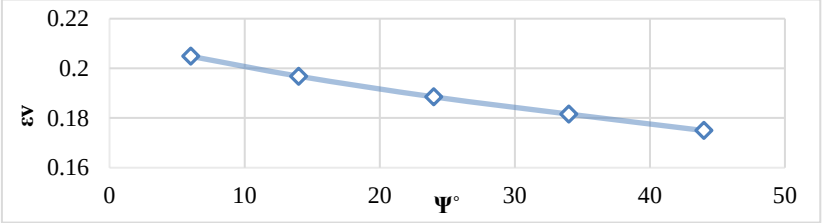

Fig. 11. The effect of changing the dilation angles of filling soil on the volumetric strain of geobag

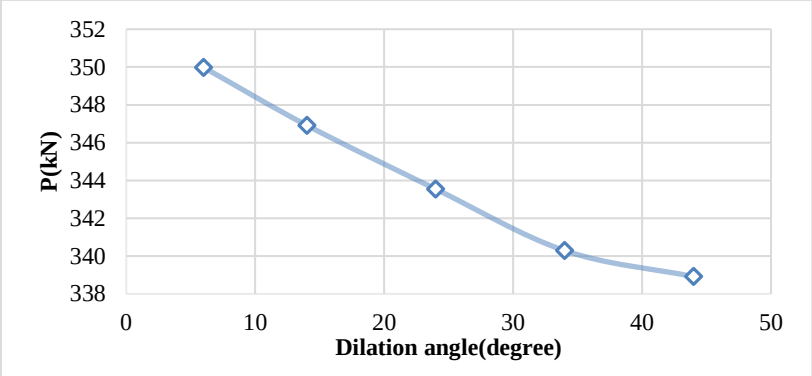

Fig. 12. The ultimate load capacity with respect to the dilation angle (peak point method)

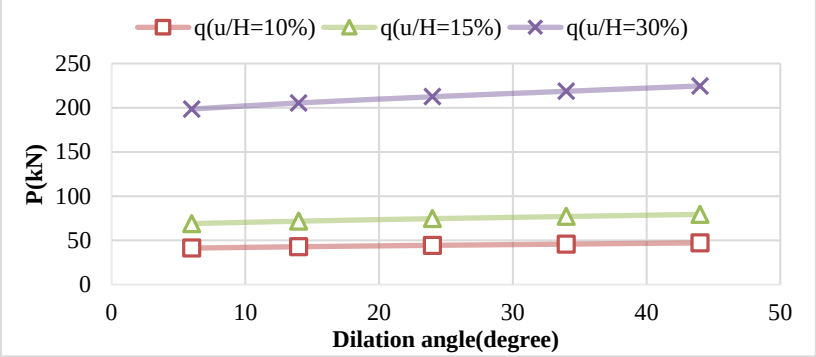

Fig. 13. The load capacity at different normal strain levels with respect to the dilation angle (u/H=10%, 15%, 30%))

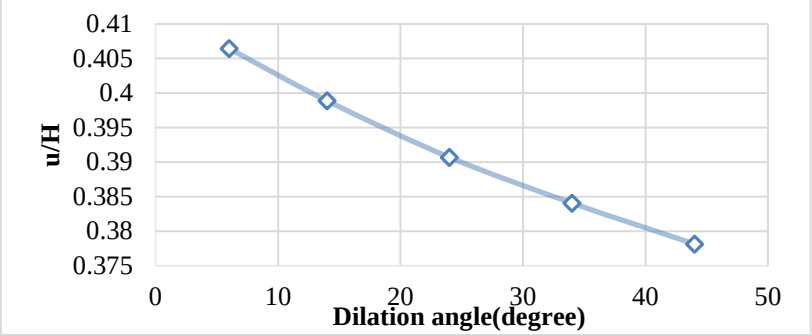

Fig. 14. The effect of the dilation angle on ultimate displacement (peak point method)

5.5 The effect of Poisson's ratio of fill soil

The change of the ultimate load and loads at different strain levels of geobag due to the increase of Poisson's ratio is demonstrated in Figs. 15 and 16, respectively. The increase in Poisson's ratio causes a decrease in ultimate load capacity as observed from Fig. 15. The increase in Poisson's ratio causes an increase in load at normal strain

levels (Fig. 16). The increase in Poisson's ratio, causes geobag's volume to increase at the higher normal strain level, which in turns causes the enlargement of the contact area of geobag with loading plate and experiencing higher pressure. Ultimate displacement of geobag declined due to an increase in Poisson's ratio of filling soil in geobag, as it is illustrated in Fig. 17. The logical explanation for this trend is that increase in Poisson's ratio is responsible for the rise in bulk modulus of filling soil, as a result, minimum decrease in geobag's volume is seen during loading conditions. This cause more stretches in geobags and increasing confining pressure. Therefore, in ultimate load condition, geobags experience less settlement.

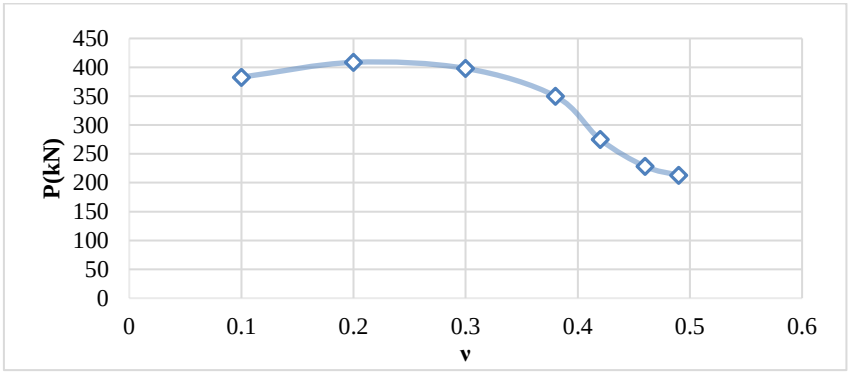

Fig. 15. The effect of Poisson's ratio on the ultimate load capacity (peak point method)

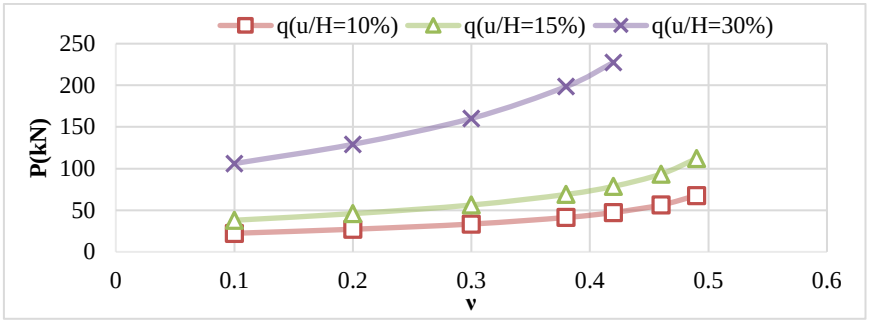

Fig. 16. The effect of Poisson's ratio on the load capacity at different strain levels (u/H=10%, 15%, 30%)

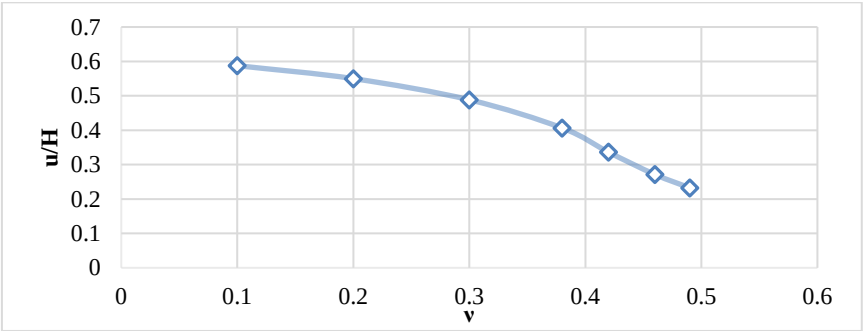

Fig. 17. The effect of Poisson's ratio on the settlement of geobag (peak point method)

5.6 The effect of modulus of elasticity of filling soil

Effect of Young's modulus of soil on ultimate load and loads at different normal strain levels is illustrated in Fig. 18 and 19, respectively. As seen, the ultimate load fluctuates with respect to changes in soil modulus of elasticity, showing the mixing effect of this parameter with other parameters used, Fig. 18. The load at higher strain levels increases due to an increase in modulus of elasticity and therefore increase in stiffness of geobags before reaching the ultimate strength, as it is demonstrated in Fig. 19. The effect of Young's modulus of soil on ultimate displacement was investigated and is shown in Fig. 20. This figure shows that much lower geobag settlement is induced to reach ultimate load capacity with an increase in modulus of elasticity. It can be argued that when the geobag is loaded, its height decreases and the length and width increase, causing the geobag material (i.e. geotextile) to stretch until it reaches its rupture strain. When the modulus of elasticity of soil is low, the volumetric strain under loading will increase. Thus, for equal vertical strain, the geobag volume will reduce and the geotextile will experience less stretching. This causes that geobag reaches its ultimate resistance at higher

vertical the strain. When the modulus of elasticity of the soil within the geobag is very low, the soil deforms more easily, thus creating a more uniform stretch in the geotextile and will cause the geobag to withstand a higher force at its ultimate strength. It can be said that on the one hand the effect of increasing the soil modulus of elasticity on the increase of the load applied to geobag at a constant vertical strain and on the other hand the effect of increasing the modulus of elasticity on the reduction of the ultimate vertical strain will cause the force, withstand by the geobag at the ultimate resistance level flactautes.

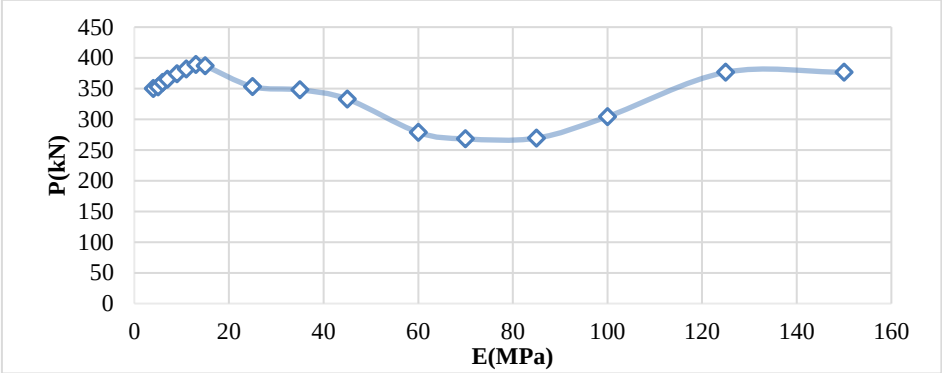

Fig. 18. The effect of soil modulus elasticity on the ultimate load capacity of geobag (peak point method)

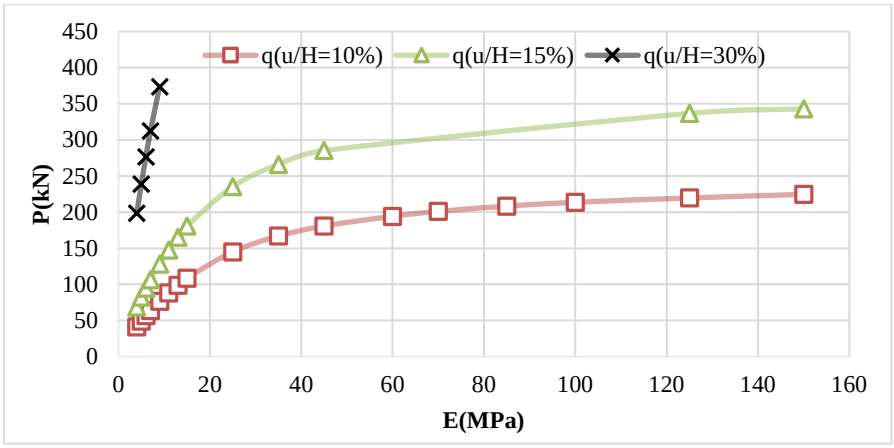

Fig. 19. The effect of soil modulus elasticity on the load capacity of geobag at different strain levels (u/H=10%, 15%, 30%)

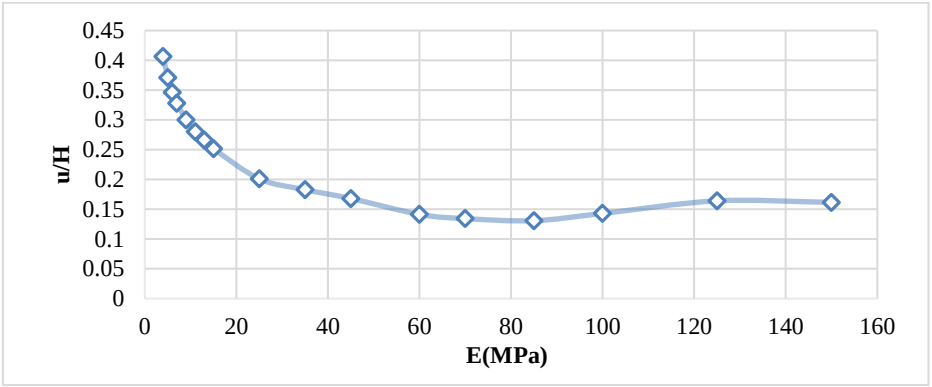

Fig. 20. The effect of soil modulus elasticity on geobag settlement (peak point method)

5.7 The effect of the tensile strength of bag material

The effects of the tensile strength of bag material on ultimate load capacity and load at different normal strain levels are shown in Figs. 21 and 22, respectively. As seen the ultimate load capacity increases with an increase in tensile strength of geotextile (Fig. 21). However, there is no noticeable change in loads at strain levels before the failure of geobag (Fig. 22). The explanation for this trend is that the tensile strength of geotextile come to affect at the end stages of loading. These findings agree with the effect of the tensile strength of bag material on geobag's

apparent cohesion presented in the previous section of this paper (equation 3). In Fig. 23 effects of the ultimate tensile strength of bag material on ultimate displacement are shown.

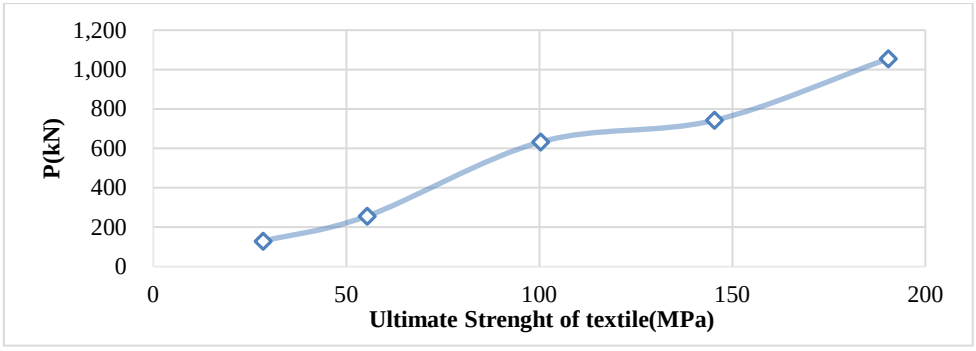

Fig. 21. The effect of the tensile strength of bag material on ultimate load capacity (peak point method)

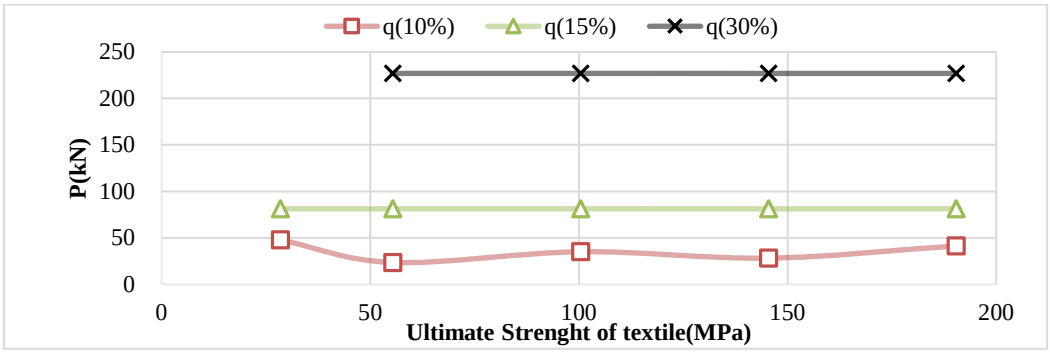

Fig. 22. The effect of the tensile strength of bag material on the load at different normal strain levels (u/H=10%, 15%, 30%)

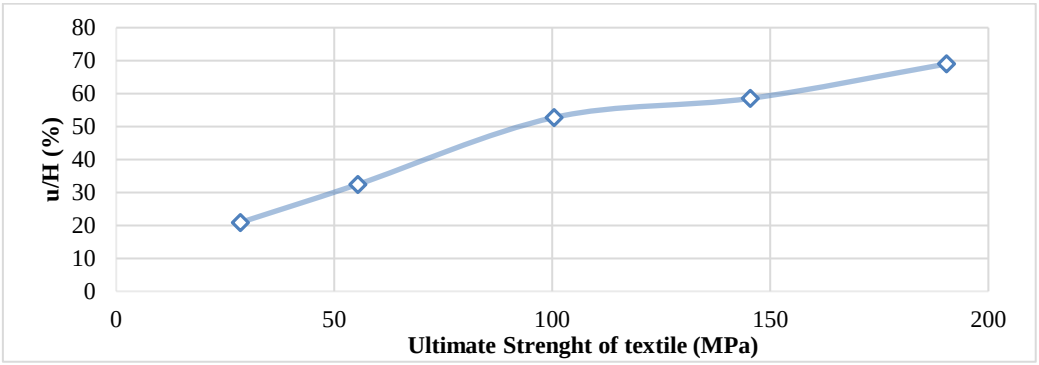

Fig. 23. The effects of the tensile strength of bag material on the ultimate settlement of geobag (peak point method)

6. Conclusions

In this paper, employing a finite element code, models of geobag were made and tested. The sensitivity of bearing capacity of geobags subjected to uniaxial loading to different properties of filling soil and bag material were investigated. These parameters included the width and height of geobag, modulus of elasticity of filling soil, Poisson's ratio of soil, soil friction and dilation angles and tensile strength of bag material. Based on the results obtained from this study, the following conclusions can be made:

1) It showed that material properties and geometrical dimensions of geobag system have significant effects on geobag's load capacity. It is therefore recommended to determine the optimum dimensions of geobag system for the materials in practice beforehand.

2) It is found that there exists an optimum width for the geobag beyond which increasing the width has no noticeable effect on load bearing capacity.

3) The results show that increasing the height of geobag leads to a decrease in the ultimate load capacity due to a reduction of confining pressure provided by the bag.

4) It is illustrated the using soils with higher friction angle will increase the ultimate load capacity and loads at different strain levels of geobags.

5) It was shown that the ultimate load of geobag decreases with increase in dilation angle of filling soil.

6) It was found that the increase in Poisson's ratio causes a decrease in ultimate load capacity.

7) The results revealed that the ultimate load capacity fluctuates with respect to changes in soil modulus of elasticity.

8) It was found that the ultimate load capacity increases with an increase in tensile strength of geotextile. It is therefore recommended to use geotextiles with higher resistance to rupture for geobag system.

Although the idea of using geobags as reinforcement elements to improve bearing capacities of weak soils is promising it suffers certain limitations and shortcomings such as the behavior when flooded, deterioration, long term deformations, environmental effect and creep that should be studied further.

7. References

[1] Kim JM, Lee DY, Oh SY. Assessment of behaviour characteristics for geobag wall system using recycled waste concrete. In: Advanced Materials Research. 2007; 26:1161-1164. Trans Tech Publications.
[2] Matsuoka H.A new interesting method of soil foundation. Kyoto University Press;2003. (in Japanese).
[3] Matsuoka H, Liu S. New earth reinforcement method by soilbags ("DONOW"). Soils and Foundations. 2003;43(6):173-188.
[4] Aqil U, Matsushima K, Mohri Y, Yamazaki S, Tatsuoka F. Application of stacked soil bags to repair and maintenance works of small earth dams. In: Proc. of Japan National Conference on JSIDRE; 2006. p. 592-593.
[5] Lohani TN, Matsushima K, Aqil U, Mohri Y, Tatsuoka F. Evaluating the strength and deformation characteristics of a soil bag pile from full-scale laboratory tests. Geosynthetics International. 2006;13(6):246-264.
[6] Xu Y, Huang J, Du Y, Sun DA. Earth reinforcement using soilbags. Geotextiles and Geomembranes. 2008;26(3):279-289.
[7] Tantono SF, Bauer E. Numerical simulation of a soilbag under vertical compression. In: The 12th international conference of International Association for Computer Methods and Advances in Geomechanics (IACMAG). Goa, India; 2008.p. 433-439.
[8] Chew SH, Pang PY, Tan CY, Chua KE. Laboratory study on the consolidation settlement of clay-filled geotextile tube and bags. Journal of GeoEngineering. 2011;6(1):41-45.
[9] Ansari Y, Merifield R, Yamamoto H, Sheng D. Numerical analysis of soilbags under compression and cyclic shear. Computers and Geotechnics. 2011;38(5):659-668.
[10] Hosseini H, Hataf N, Talebbeydokhti N. CFD modeling of geomat protected abutments.In: 5th Asian Regional Conference on Geosynthetics. Bangkok, Thailand; 2012.
[11] Hataf N, Sayadi M. Experimental and numerical study on the bearing capacity of soils reinforced using geobags. Journal of Building Engineering. 2018;15:290-297.
[12] Liu S, Fan K, Xu S. Field study of a retaining wall constructed with clay-filled soilbags. Geotextiles and Geomembranes. 2019;47(1):87-94.
[13] Chen Y. Deformation and strength properties of a 2D model soilbag and design method of earth reinforcement by soilbags. Report to Venture Business Laboratory, Nagoya Institute of Technology. 1999. (in Japanese).
[14] Pu M, Liu S, Zhu K. Experimental study on an expansive soil and its containment in bags under drying-wetting cycles. College of Water Conservancy and Hydropower Engineering, Hohai University, Nanjing. 2008. (in Chinese).
[15] ABAQUS/Standard User's Manual, Hobbit, Karlsson &. Sorensen, Inc., Pawtucket, Rhode Island;2002.